SUPPLEMENTARY FIGURES

Cav3.2 T-type calcium channels shape electrical firing in mouse Lamina II neurons

Miriam Candelas [1,2,3,4], Ana Reynders [5], Margarita Arango-Lievano [2,3,4], Christoph Neumayer [1,2,3,4], Antoine Fruquière [1,2,3,4], Elsa Demes [1,2,3,4], Jawed Hamid [6], Céline Lemmers [1,2,3,7], Claire Bernat [1,2,3,7], Arnaud Monteil [1,2,3,4,7], Vincent Compan [1,2,3,4], Sophie Laffray [1,2,3,4], Perrine Inquimbert [8], Yves Le Feuvre [9], Gerald W. Zamponi [6], Aziz Moqrich [5], Emmanuel Bourinet [1,2,3,4*], Pierre-François Méry [1,2,3,4 *]

ACGCGTTCAAGGCTCAAGGCTCTTCCTGATCCCTCTCCTGGGTGGCTAGGTCCTTAATTGCTCTTTGA

MLUI

GGACCTTAATTATGGGCCGCAGCCACCCACTGGTAAGTAGGAGCATTAAAATAGAGTAAATGTTTTTC

TTTTCTTGAAAAGTTCACATATACAAGACAAGGTGCTGTTGGGCCCAGGGGCCTGCCCTGCCTGGACC

GACAGGCAGAGGACATGGTTCTTGTTCTCCACCTCCTTCCCCAGGCTGTGCCCTTCCCAGGCTCAGTG

GTGAAATCCTCTTAGAATCCCAGAACCACATATGGGAAACTCCACTTCTCTGCAGCTCACCCTGCCAG

GGCTCCATCCAGGTCTGAGGTTGCTATGTTGCTCTGGCCCTCCAAAGAGCCCAGCTACCCCAGGGCAG

AGGGAGGCTGCTCTTTGTCTAGGACAGGAATGGTTTTCCCCAATAACAGGGCCTGAAGGTGAAAGAGC

CCCTTGTTGGTTGAAATTTAAGTGGATGTACACCTAAGAGCTGGAATTTTATGGCCCTAGTGTGGTAA

TTGTGAGAAAGTAAAAAAATCCCTGCATACCTCCAGCGGGAGAGGGGGGGAACAGCCCCTCTGCTCAT

GCCTTCATGGGACAAGGGTCATGCAACCACTGGAGTATGAAAGGAGATTCAGCGACATGCTCAGGATA

TACCCTCTGTGTGCCTTGGCGGGTGCTGGGAGGCCCCGCTCGGCTTGTACTCCTTCTCGAGGTTCTTC

CAAGAGCCCCAGTCCCCAGGAGAAGGGGGAGGGGGATGGGCACCGGCAAGTTTGCGGAAACTGGGAGG

AGTGTGGGGGAGCTGCGTACCAGAGTACCCGGACTGCCCCAGGACAATTGGTGTCGCGTCGCGCAACG

CGCCCCACGTCGCCCACGCGCCCCAAAGACACTGGCGCCCCGGCACACCCAAGACACACGCGGTGGGG

GAAGGGCACGCGCCTCGCGGGCATGGTCACGGCGTGCCTCCCACGCCTGCTGAGCCCCGCCCCCTAGC

CGACCCTAGCAGTGAAGAGAAGGGGCGGCGCGCGAGAAAAGGAGGGGGTCCCCGCCGGCTCCGCGCCC

CCGCAGTGGGGGTGGGGAAGGACGTTGGCGCCGCTTCCCCCGCCCCTCGTCCAAGCATCCCTGCGAGC

GCCCCCTGCTGCCGTGCTCTCCCGCGAGACAGTATGGGGCGGGAGGAGAGGTCGGGGAGGGGGGCGCG

GACCGGGTTCGCCCAGTCCTGGACTTGGGGCTGGCGGCGTACCGGCACGGAGAAACACGGACCAAGGG

ATGTTGTGGGATAGCTTACGTCTGGGTGGGGGCGGGCCGGGCTGATGACCCCCGCCCACTCTCCGTCC

CTATCTCGGTCCCTGAGGGTCGCCCCCTGCCCGCCCCGGCCGCGTTGGCCCCGCCCCATGGGCCGCCC

CCGCCGCCCCGCCTCCCCGCCACTGCTCACTCCGAAGTTT***GGATCC***

BAMHI

Supplementary Figure S1. Minimal mouse Cav3.2 promotor sequence of the AAV constructs. Core promoter is presented in bold capital letters flanked with extra MluI and BamHI sites (in italics) used for cloning.

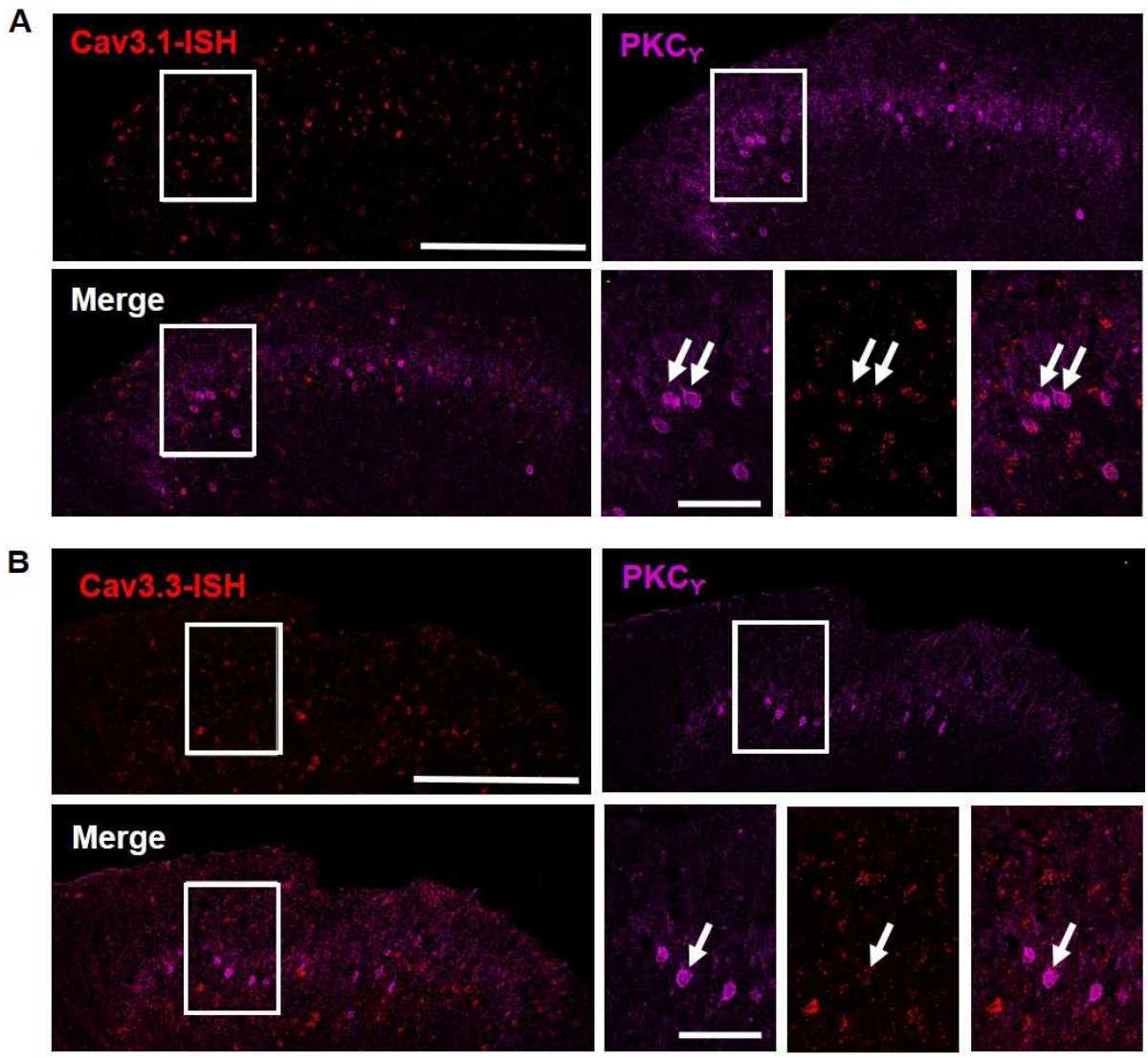

Supplementary Figure S2. PKCγ neurons express Cav3.1 and Cav3.3 in the dorsal horn of the spinal cord of adult mice. (A) Sections of spinal cord at the lumbar level demonstrating overlaps in the expression of Cav3.1 mRNA (red), by means of *in situ* hydridization (see Table 2 for probe sequence), and of PKCγ immunoreactivity (blue) detected with a rabbit anti-PKCγ.and amplified with a donkey anti-rabbit A647 antibody. **(B)** Same as in **(A)** except that the Cav3.3 (red) was revealed by *in situ* hybridization. Arrows in **A** and **B** show coexpressions of markers. Scale bars: **A, B** (long=200µm, and short=50µm).

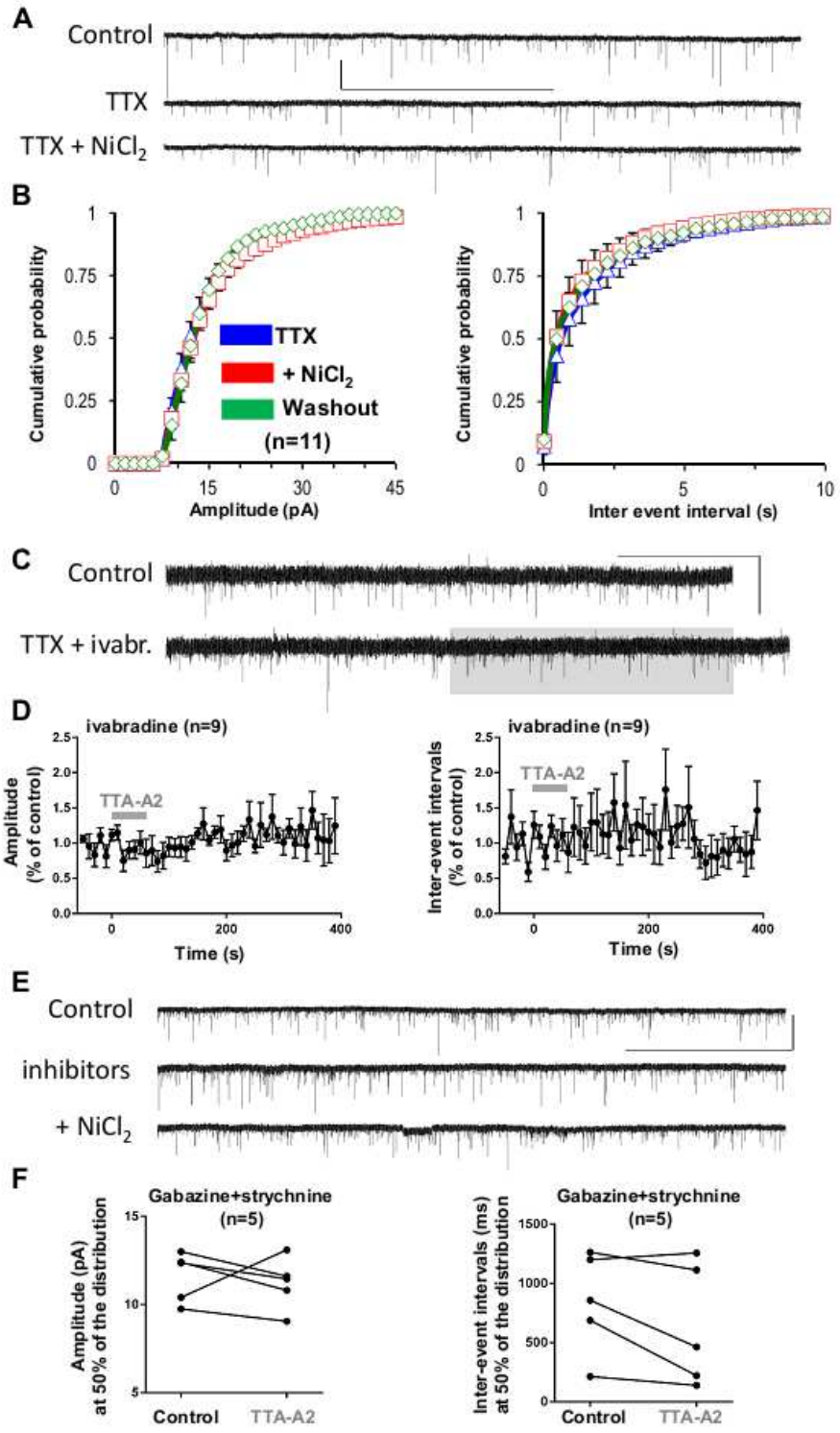

Supplementary Figure S3. T-type calcium channels do not control the mean excitatory neurotransmission of LII neurons in the spinal cord of adult mice. (A) Excitatory synaptic currents recorded successively under control conditions, in the presence of TTX 500 nM and in the presence of TTX + $NiCl_2$ 100 µM in a LII neuron held at -70 mV. Note that TTX diminished the synaptic activity, which was not altered further by $NiCl_2$. Scale bars: 40 pA, 1 min. (**B**) Mean cumulative distributions of the amplitudes (**left panel**) and the inter-event intervals (**right panel**) of mEPSC in the

absence (TTX 500 nM) or during the superfusion with 100µM $NiCl_2$ (n=11). **. (C)** Excitatory synaptic currents recorded in a LII neuron held at -70 mV, under control conditions, and in the presence of TTX 500 nM + ivabradine 1 µM, a HCN inhibitor (see Huang et al., 2011), without or during ejection of 1 µM TTA-A2 (shaded area). Scale bars: 40 pA, 30 s. **(D)** Mean amplitudes **(left panel)** and inter-event intervals (**right panel**) of mEPSC before, during and after a 1 min-long ejection of 1µM TTA-A2 (start at time 0) in the continuing presence of ivabradine 1µM (n=9). Data are shown as series of 10s-long bins, normalized to the levels recorded before TTA-A2 ejection. **(E)** Excitatory synaptic currents recorded successively under control conditions, in the presence of TTX 500 nM + Gabazine 3 µM + strychnine 3 µM, without or with $NiCl_2$ 100 µM in a LII neuron held at -70 mV. Note that the inhibitors increased inter-event intervals, while $NiCl_2$ had a marginal effect on the synaptic activity. Scale bars: 30 pA, 40 s. **(F)** Midpoints of the cumulative distributions of the amplitudes **(left panel)** and the inter-event intervals (**right panel**) of mEPSC in the absence (control) and during the superfusion with TTA-A2 500nM in 5 separate experiments performed in the continuing presence of Gabazine 3µM and strychnine 3µM, respectively inhibitors of GABA-A and glycine receptors.

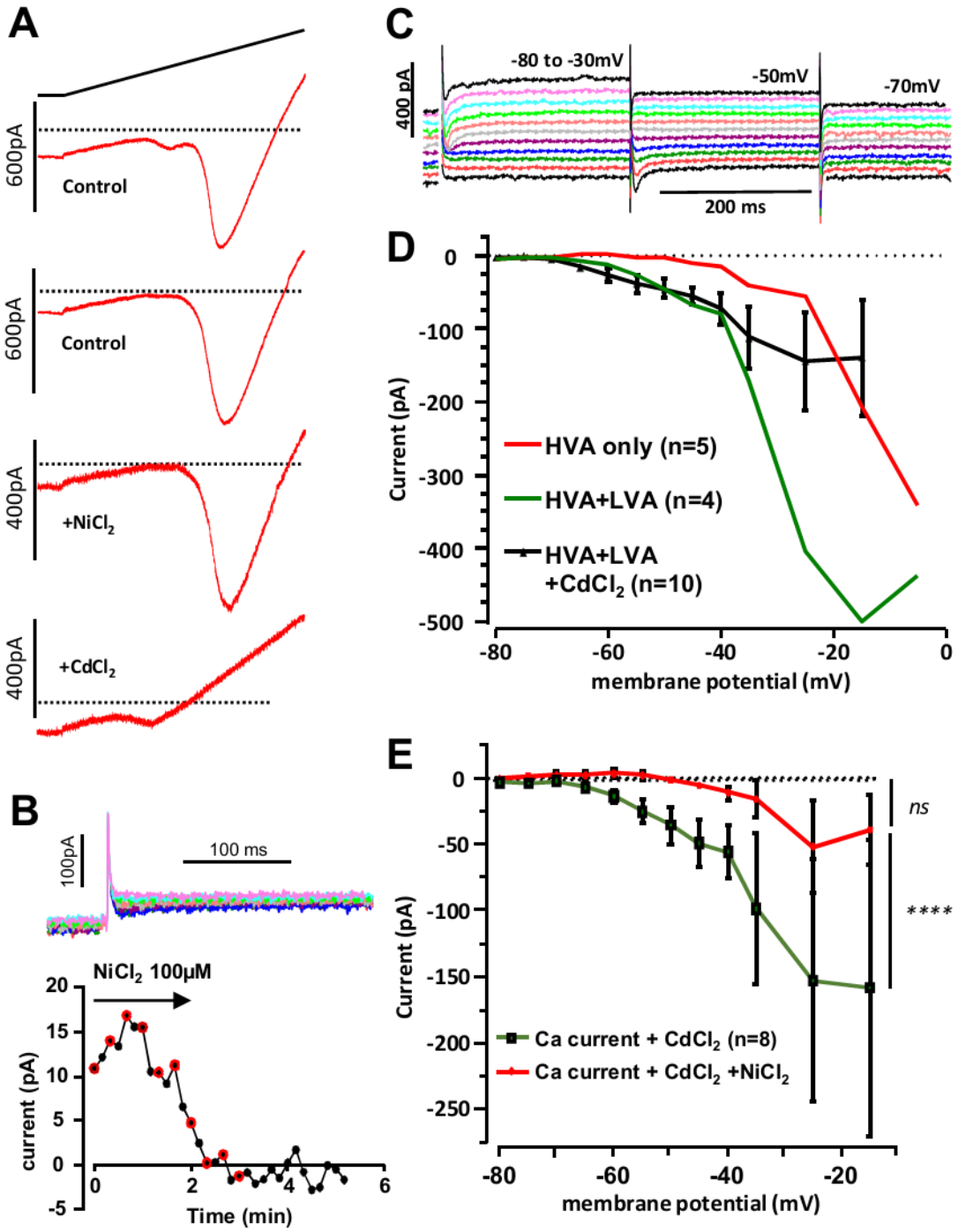

Supplementary Figure S4. T-type currents of LII neurons in the spinal cord of adult mice. (A) Voltage ramp relationships of four different LII neurons recorded under control conditions and in the presence of either 100µM $NiCl_2$ or 100µM $CdCl_2$. The dotted line shows the 0 pA level. The 200ms-ramp is indicated by the upward-going line. **(B)** Typical experiment in a LII neuron where the inward current recorded at -65 mV from a holding potential of -90 mV was inhibited by the superfusion with 100µM $NiCl_2$. The superimposed current traces are taken at the times indicated by the red symbols. **(C)** Family of current traces elicited by step-depolarisations (5mV increments) in a LII neuron from a holding potential of -90mV. Traces were shifted step-by-step to the top, for clarity. **(D)** Mean current-

voltage relationships of LII neurons (protocols as in **C**) recorded in the absence (colored lines) and presence (black line and symbols) of 100µM $CdCl_2$. Neurons without low-voltage activated inward currents (red line) are compared with neurons exhibiting both low- and high-voltage activated currents (green line, and black symbols) **(E)** same as in **D** except that the calcium current remaining in the presence of 100µM $CdCl_2$ was inhibited by 100µM $NiCl_2$. *ns*, non significant; ***, $p<0.005$, using a Wilcoxon paired test. **(A-E)** all recordings were performed in the presence of extracellular DNQX (20µM), APV (50µM), and Gabazine (3µM). In **D** and **E**, squares and vertical lines are for the means and the SEM. See Methods for additional information.

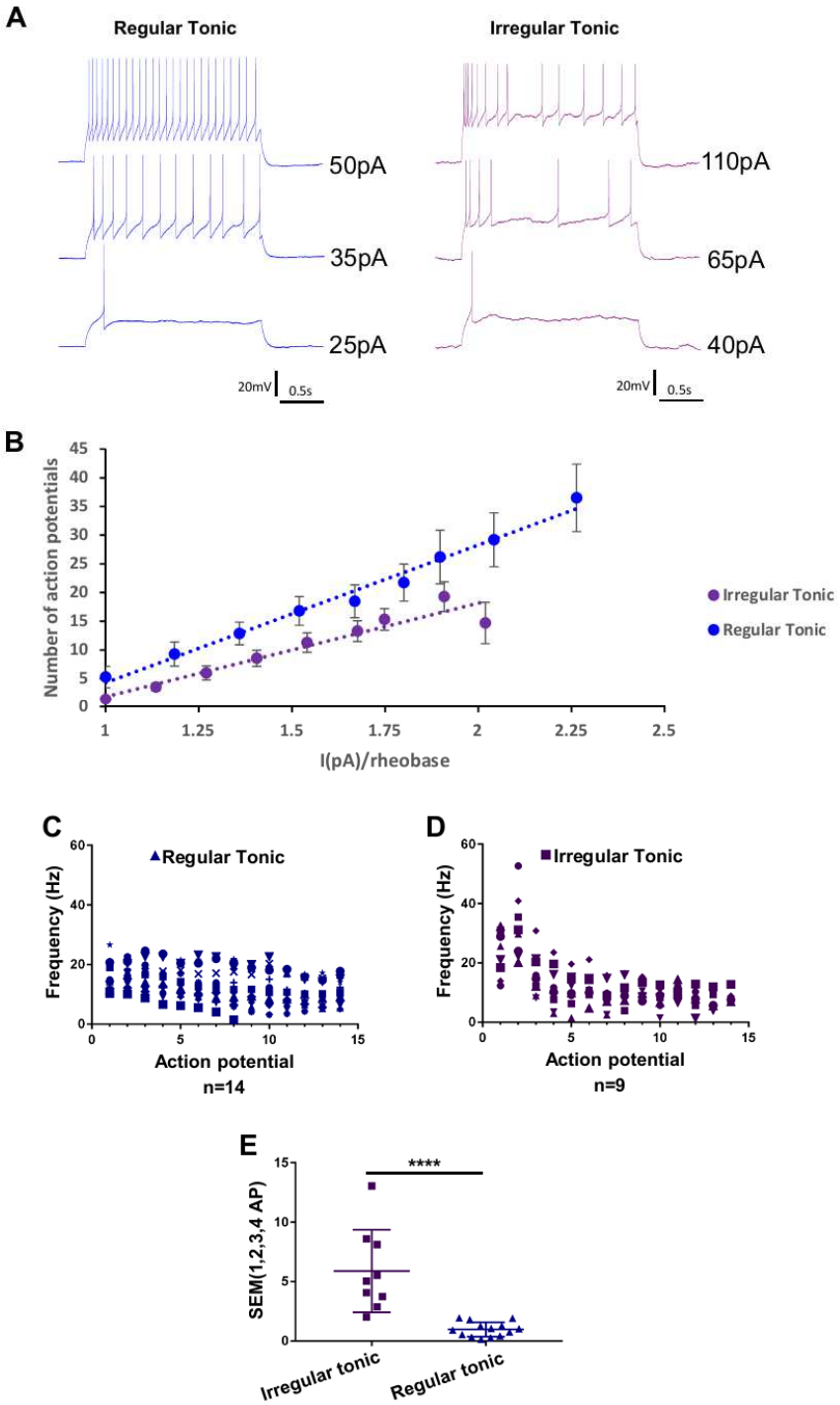

Supplementary Figure S5. LII neurons displayed two types of tonic firing patterns in adult mice. **(A)** Typical recordings of regular tonic and irregular tonic firing patterns at three current injection amplitudes. **(B)** Mean number of action potentials (elicited during a 2 sec-pulse, see Methods) as a function of the ratio (amplitude of the stimulatory current / rheobase) in tonic LII neurons. Note that 1) regular tonic neurons (n=10) are more active than irregular tonic neurons (n=14) and 2) the relationship is more likely linear (dotted line, r^2=0.98) in the regular tonic subpopulation as compared to the irregular tonic subpopulation (dotted line, r^2=0.91). **(C,D)** Instantaneous frequencies of the first 15 action potentials elicited by current injections in different neurons. **(E)** Calculation of the SEM of the frequency of the first 4 action potentials is sufficient to discriminate between regular and irregular tonic regime in LII neurons. Lines are means and SEM, and dots are the individual values. **** $p<0.0001$ using a Mann-Whitney test.

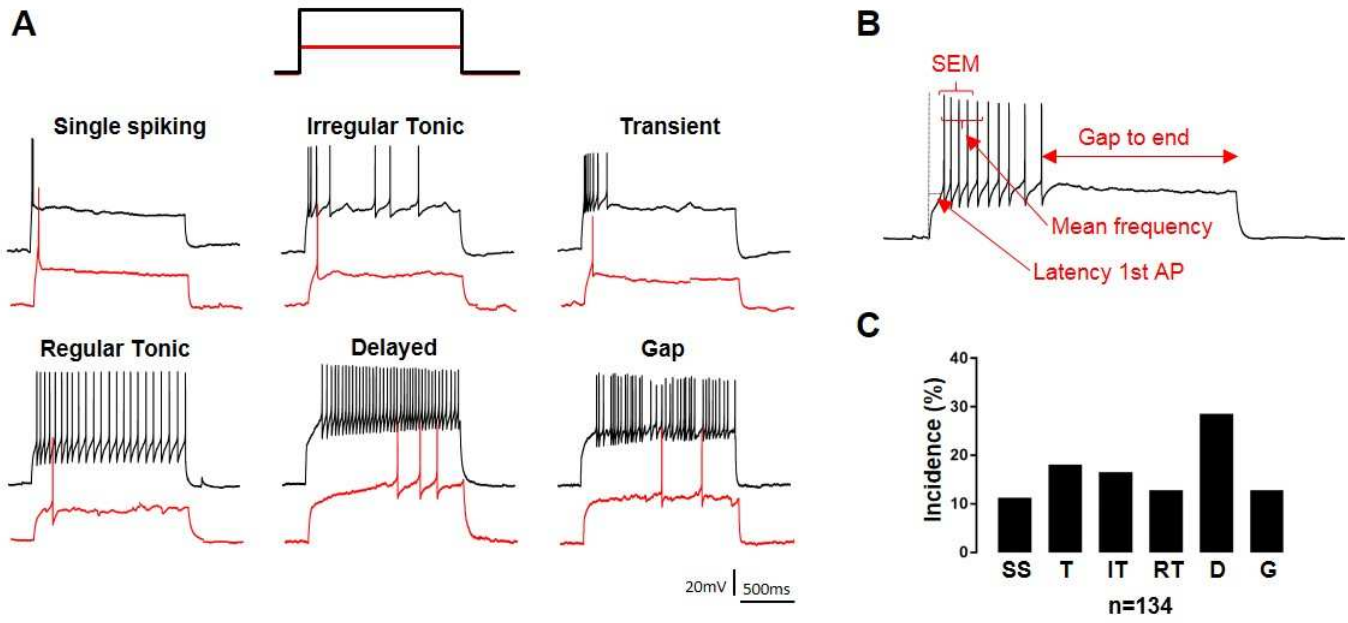

Supplementary Figure S6. LII neurons displayed different types of discharge profiles. (A) Individual traces of the firing patterns in LII neurons in adult mice. Current injections were performed after setting a resting potential at -70mV. Red traces are the activity at rheobase, and black traces are the activities at steady state regime. **(B)** Parameters allowing the classification of firing patterns of LII neurons. SEM (Standard error of the mean), AP (Action potential). **(C)** Graph showing the proportions of neurons expressing different profile discharges (n=134). SS (Single spiking: less than 2 action potentials per pulse), T (Transient: activity duration < 1.4s in a 2s-long pulse), IT (Irregular Tonic: tonic and having a SEM of the first 4 action potential intervals >2), RT (Regular Tonic: tonic and having a SEM of the first 4 action potential intervals <2), D (Delayed: the latency of the first action potential >95ms and a mean frequency of the first 5 actions potentials >8Hz) and G (Gap: the latency of the first action potential >95ms and a mean frequency of the first 5 action potentials <8Hz).

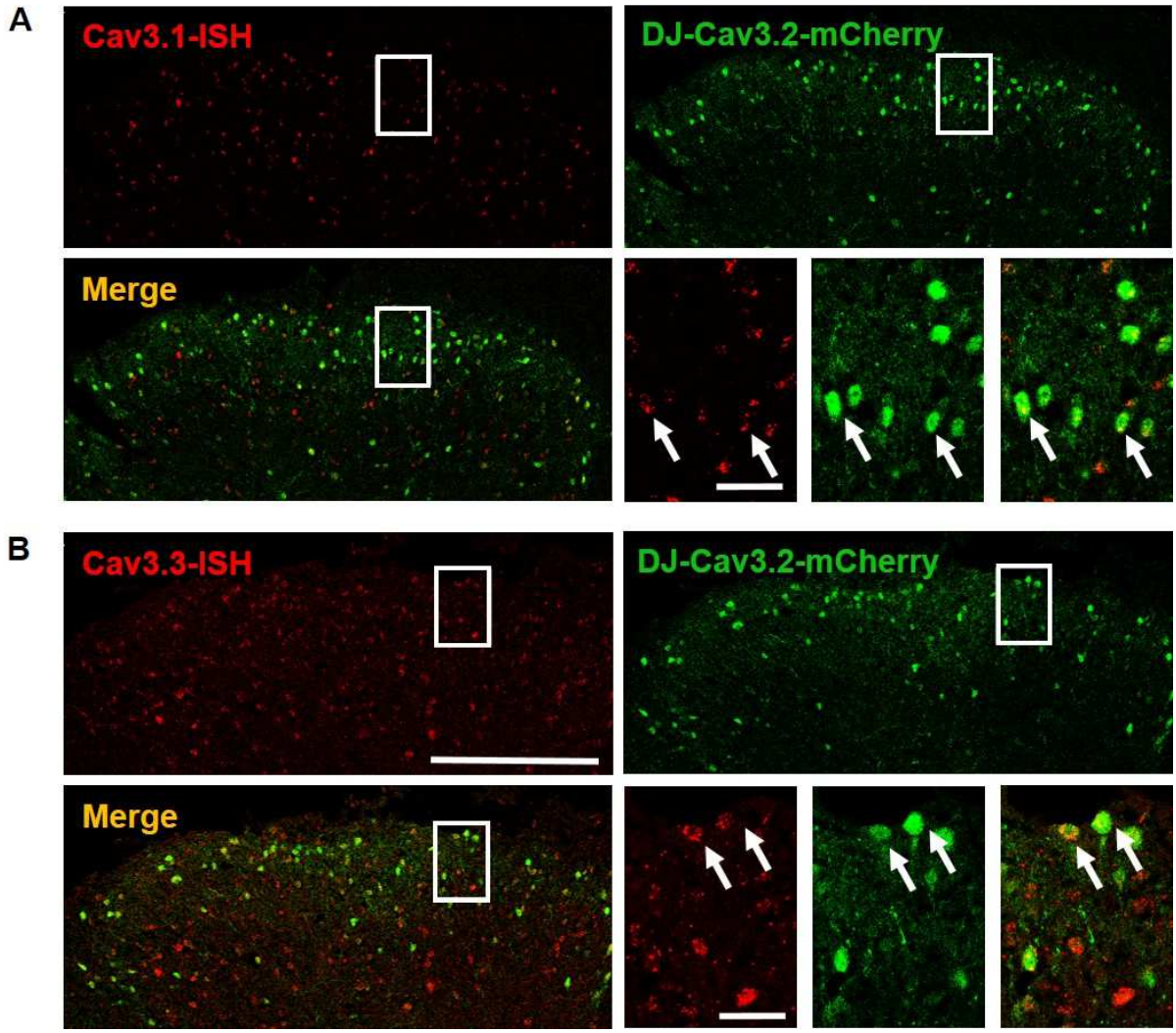

Supplementary Figure S7. Cav3.2-mCherry neurons expressed Cav3.1 and Cav3.3. (A) Colocalization of Cav3.1 mRNA (red, supplementary Table S2 online, for probe sequence) by *in situ* hybridization and mCherry (green) by immunodetection in wildtype mice injected with AAV-Cav3.2-mCherry. mCherry was detected with an anti-GFP antibody (supplementary Table S1 online). Arrows show coexpressions. **(B)** same as in **(A)** except that Cav3.3 mRNA was targeted by *in situ* hybridization. Data representative of 3 mice. Scale bars: **A,B** (200µm, 25µm).

References:

Huang, Z., R. Lujan, I. Kadurin, V. N. Uebele, J. J. Renger, A. C. Dolphin and M. M. Shah (2011). "Presynaptic HCN1 channels regulate Cav3.2 activity and neurotransmission at select cortical synapses." Nat Neurosci **14**(4): 478-486.